Int J Adv Manuf Technol (2017) 88:291–301
DOI 10.1007/s00170-016-8754-6

ORIGINAL ARTICLE

Hydrostatic radial forward tube extrusion as a new plastic deformation method for producing seamless tubes

S. S. Jamali[1] · G. Faraji[1] · K. Abrinia[1]

Received: 29 December 2015 / Accepted: 7 April 2016 / Published online: 23 April 2016

Abstract Hydrostatic radial forward tube extrusion (HRFTE) as a new and innovative method is developed for producing large-diameter seamless tubes from smaller hollow billets. The HRFTE process is based on hydrostatic pressure, and radial forward tube extrusion provides the possibility of producing a large-diameter tube with low hydraulic oil pressures. In this procedure, a movable punch placed inside the hollow billet plays the main role in reducing the required hydrostatic pressure. The HRFTE process was applied to pure aluminum at room temperature, and the mechanical properties, material flow behavior, and microstructural evolution were examined. Since the large effective strains were applied to the material during the process, the strength and hardness were significantly improved. Yield and ultimate strength were increased, respectively, about 2.48 and 1.86 times compared to the initial values. Microhardness was also increased to 59 Hv from the initial value of 28 HV. Good homogeneity of effective strain and microhardness in the longitudinal section was observed, but there is an inhomogeneity along the tube thickness. The HRFTE process seems to be an extrusion process with a high capability of industrialization for producing a large-diameter seamless tube with superior mechanical properties using low hydrostatic pressures.

Keywords Radial forward extrusion · Hydrostatic pressure · Mechanical properties · Aluminum · Effective strain

✉ G. Faraji
ghfaraji@ut.ac.ir

[1] School of Mechanical Engineering, College of Engineering, University of Tehran, Tehran 11155-4563, Iran

1 Introduction

In the production of industrial parts using metal-forming processes, extrusion is one of the most important methods. Considering the directions of the material flow and punch movement, extrusion processes are divided into three categories of forward (direct), backward (indirect), and radial (lateral) extrusion. The combination of two or three of these processes is named as a combined extrusion method. Some methods of combined extrusion are double backward extrusion [1], backward forward extrusion [2], radial backward extrusion [3], and radial forward extrusion [4]. Hydrostatic extrusion, patented by Robertson in 1893 [5], has several advantages over conventional extrusion including almost no friction, lower process load, better surface quality, and higher hydrostatic compressive stress (essential for processing hard-to-deform materials) [6]. Bridgman in 1952 carried out several experiments in the design and construction of the pressure chamber which is an important part of the system [7].

Among the extrusion products, seamless tubes are used extensively in different industries. Production of the seamless tubes is conventionally performed by using piercing forward extrusion, backward extrusion [8], and port-hole methods [9]. During the last decade, several tube severe plastic deformation (SPD) methods with applying intense plastic strain leading to significant grain refinement were invented for improving the mechanical properties of the tubular-shaped metals [10–12]. Faraji et al. [13, 14] introduced tubular channel angular pressing (TCAP) [15] and parallel tubular channel angular pressing (PTCAP) processes for producing ultra-fine-grained (UFG) tubes. Babaei et al. developed tube cyclic expansion extrusion (TCEE) [16]. These processes may be used only for small tubes on the laboratory scale [17]. Whereas the long and large tubes are demanded in industries, development of effective methods is necessary. Scaling up of the available SPD process

may be impossible because of its limitations [18]. Requiring of a vast amount of force is a significant problem in conventional extrusion. Besides, in most of the SPD methods, an increase in the diameter or length of the tube [19] leads to buckling or yielding of the pressing punch.

In the present paper, a new and innovative method called hydrostatic radial forward tube extrusion (HRFTE) process with the possibility of producing seamless tubes while using low hydraulic pressures is provided. To investigate the capability and applicability of the process, a commercial Al tube is processed and the mechanical properties, material flow behavior, and microstructural evolution were examined. The finite element method (FEM) is also used to study the deformation behavior.

2 Principles of the HRFTE

A schematic of the HRFTE process is shown in Fig. 1a–c. The HRFTE process is performed based on a combination of conventional radial forward extrusion and hydrostatics benefits in which there is almost no contact friction between billet and the die. The initial billet is a tube with a smaller diameter and greater thickness compared to the final tube at the end of the process. The initial billet constrained by the mandrel and a movable punch is placed inside the outer die (Fig. 1a). As can be seen in Fig. 1a, hydraulic fluid fills the space between the initial billet and the primary pressure container, which by eliminating the friction force reduces the force required for the process [20, 21]. The movable punch is moved simultaneously with the initial billet during the process. As shown in Fig. 1b, a hollow billet is extruded into the annular gap until it reaches the tube outer diameter. Then, the material is extruded into the annular 90° channel and the tube forms around the mandrel, and a larger-diameter tube is produced from the initial small-diameter billet. As well, simultaneous use of the movable punch inside the initial billet and hydraulic fluid increases the effective area and consequently a significant reduction in the required fluid pressure is achieved. According to the Pascal principle, the pressure is inversely proportional to the square of the punch diameter.

Simultaneous use of the movable punch and the hydraulic fluid causes an increase in the effective area. Thus, when processing large-diameter tubes, the rate of deformation force increase is not greater than the rate of effective area rise. So, the required hydrostatic pressure is constant or reduced by increasing the tube diameter. In fact, in the conventional processes, increasing the diameter of the initial billet increases the power requirements and involved limiting the production of seamless tubes with large diameters. In the present method, a possibility for the production of large-diameter seamless tubes is provided because the process could be done at low hydrostatic pressures.

3 Experimental and FEM procedures

In the present work, a commercially pure aluminum (99.5 %) was employed in the tests. A hollow billet of 22 mm outer diameter, 4 mm thickness, and 35 mm length was machined from a rolled plate and then annealed at 400 °C for 2 h. A hydrostatic radial forward tube extrusion pressure container, a punch, a mandrel, and other components were manufactured from tool steel and hardened to ~55 HRC. MoS_2 spray lubricant was used on the die set surfaces in the deformation zone to reduce the friction in the particular contact area [22]. Geometrical parameters for the HRFTE die are shown in Fig. 1d. Die parameters are as follows: $R_1 = 12$ mm, $R_2 = 11$ mm, $R_i = 13.5$ mm, $R = 16$ mm, $R_{d1} = R_{d2} = R_m = 1.5$ mm, $H = 3$ mm, and $\alpha = 15°$. As shown in Fig. 1a, the primary channel of the die was used as a pressure container that is filled with hydraulic oil, and a cylindrical punch transmits the force of a press into the fluid chamber [20, 21, 23]. A small tungsten carbide (WC) piece with a precise dimension and close tolerances with one piece of polytetrafluoroethylene (PTFE) with a bit larger diameter was used as the seal material. Hydrostatic pressure in the container increased by applying force to the cylindrical punch by a hydraulic press. The tests were conducted at a ram speed of about 5 mm/min at room temperature.

Microhardness of the samples was measured at cross sections both parallel and perpendicular to the tube axis with a load of 100 g applied for 10 s. Tensile properties of the unprocessed billet and processed tubes were investigated using the tensile test at room temperature at a strain rate of 10^{-4}. Gauge length, gauge width, gauge thickness, radius length of grip section, and width of grip section of the tensile test samples were, respectively, 15, 5, 2.5, 2.5, 40, and 10 mm. Standard metallography and optical microscopy (OM) were used to study the material flow pattern and the microstructure of the samples [24].

The HRFTE process has been simulated by the FEM to inquire into the deformation behavior during the process. Due to the symmetry of the process, axisymmetric Deform-2D simulation was conducted. The geometrical dimensions of the die component and specimen and also mechanical properties in the simulation of the process were considered to be identical to the experiment. One thousand four hundred square mesh elements with four nodes and an edge length of 0.5 mm were used to mesh the model. The tube is considered as a deformable part while all the die parts are considered as rigid bodies. Also, an automatic remeshing method was employed to adapt the imposed large strain and increase the accuracy of the results. The Coulomb friction coefficient was assumed to be 0.05 between all die components and the billet except between the primary channel of the die and the initial billet [25]. The interaction between the primary channel of the die and the initial billet is considered frictionless because of the used oil to model the hydrostatic pressure medium.

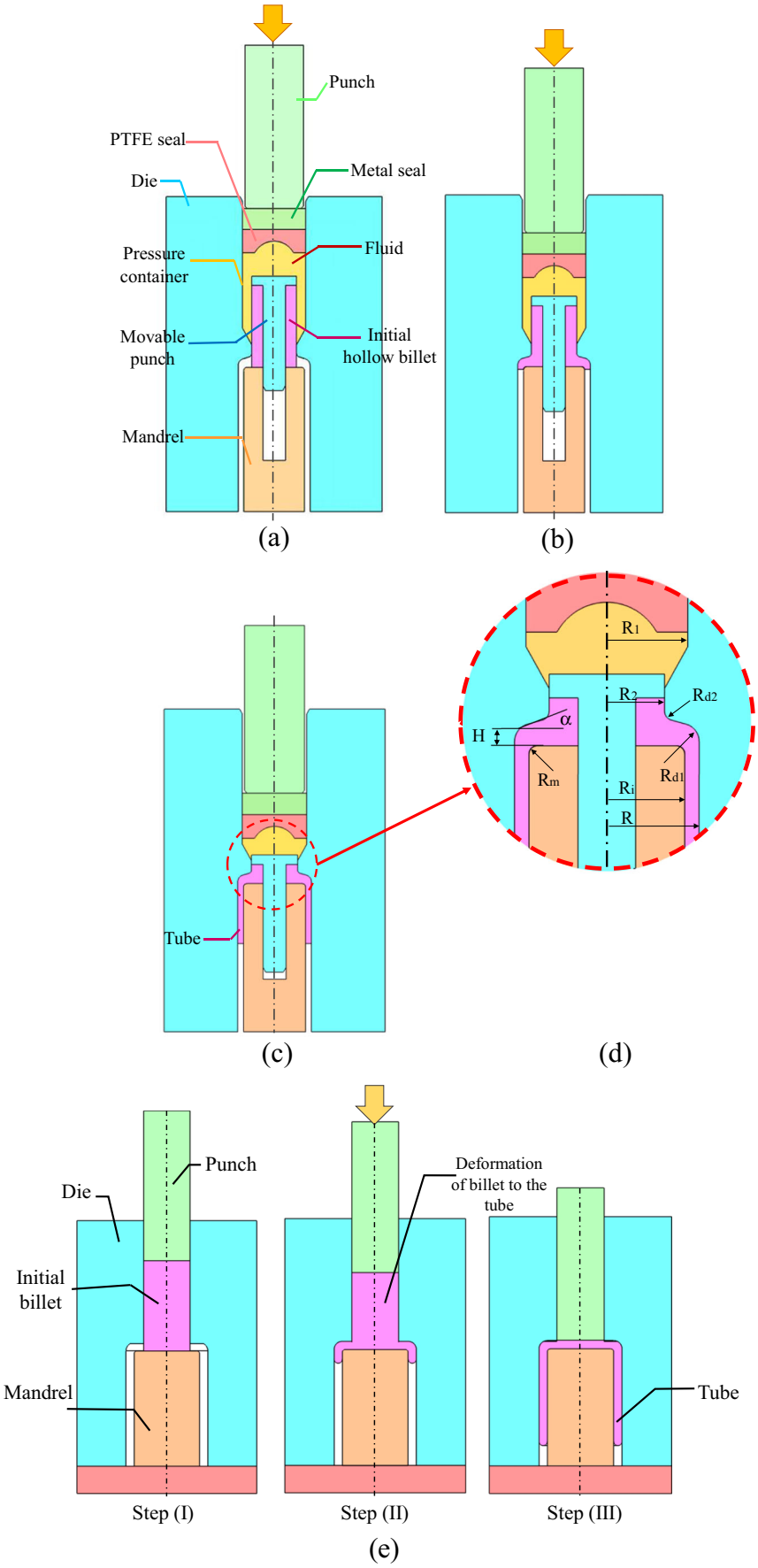

Fig. 1 Schematic of the HRFTE process **a** at the start of the process, **b** during the process, and **c** at the end of the process; **d** die parameters; **e** schematic of the conventional radial forward tube extrusion (RFTE) process

4 Results and discussion

Figure 2 shows the unprocessed hollow billet and the final processed tube formed around the mandrel at the end of the HRFTE process. As shown, a thick-walled tube with a smaller diameter becomes a seamless thinner tube with a larger diameter during the HRFTE process. Also, the length of the formed tube with good surface appearance is longer than the initial billet because of the thickness reduction.

As mentioned, the mechanism of the piston pump was used to provide hydrostatic pressure in which a cylindrical rod transmits the force from the hydraulic press to the pressure container. According to the Pascal principle, hydrostatic pressure is the result of force required divided by the effective area. Figure 3 shows the experiment and FEM calculated required force versus ram displacement during the HRFTE process. As shown, the force curve of the HRFTE process consists of four zones. In the first zone, the force increases until the material reaches its flow stress. Then, the material enters the radial channel with an increase in the force level. In this zone, the slope of the curve is changed. The third zone started at the start region of the second channel corner. In this zone, the force is sharply increased so that the material fills the corner gap. The slope is larger than that of the previous zone. When the corner gap is filled, the last zone started at the pick load. The highest force occurs at the end of the radial channel and entry of the forward channel. As represented, there is a good agreement between the experimental and FEM calculated curves. The maximum forces of the experimental and FEM are, respectively, about 67.9 and 71.1 kN. The linked hydrostatic pressures to these loads are, respectively, about 1787 and 1871 bar. The highest difference between the two curves is 4.4 %.

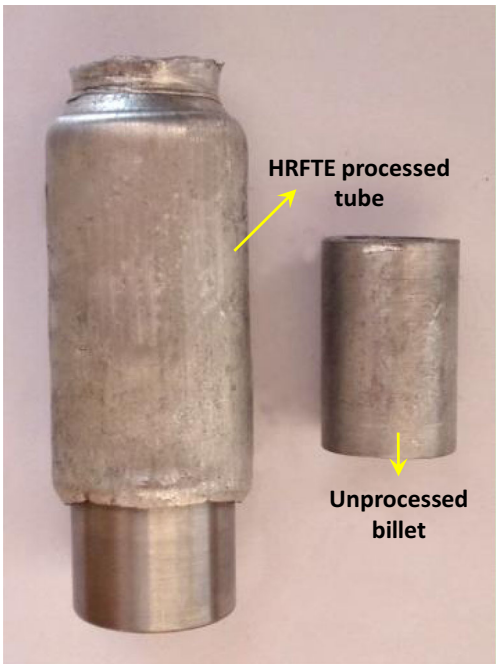

Fig. 2 A workpiece from the initial hollow billet changes to a larger-diameter tube around the mandrel at the end of the HRFTE process

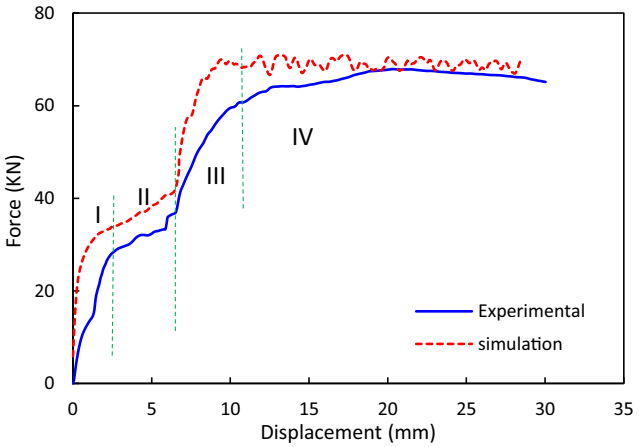

Fig. 3 Experimental and FEM calculated force versus ram displacement during the HRFTE process

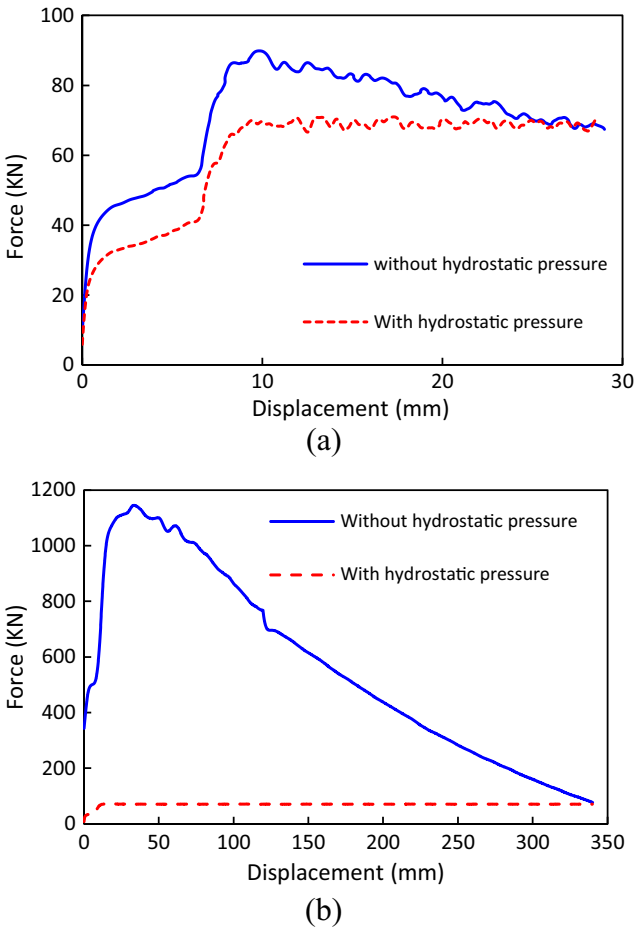

Fig. 4 **a** FEM calculated force versus ram displacement during the HRFTE process with and without hydrostatic pressure for a 35-mm-long tube. **b** Force versus ram displacement during the HRFTE process with and without hydrostatic pressure for a 350-mm-long tube

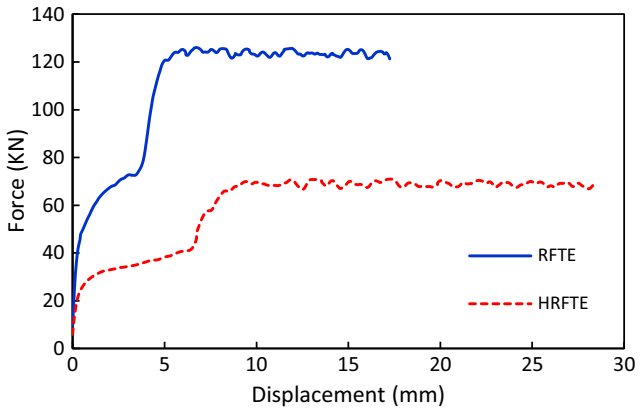

Fig. 5 FEM calculated force versus ram displacement for the HRFTE and conventional radial forward tube extrusion processes

Using the hydrostatic pressure mechanism in the HRFTE process, in which a hydraulic fluid exists between the primary channel walls of the die and initial billet, eliminates the friction in this region. With the elimination of the friction force, the required total force is reduced [20, 26] especially in the case of longer or large-diameter billets. Generally, by increasing the contact area between the wall of the initial billet and the die, the reduction is more significant [17]. The curves in Fig. 4a, b illustrate this issue clearly. Figure 4a shows the force diagrams for the HRFTE process with and without the hydrostatic pressure. The maximum forces for these procedures are, respectively, 71.1 and 89.9 kN. The use of hydrostatic pressure reduces the amount of force required about 20.9 %. However, this difference may highly increase when processing long billets. Figure 4b shows the FEM calculated force versus ram displacement during the HRFTE process with and without hydrostatic pressure for the 350-mm-long tube (10 times longer). The radial forward tube extrusion (RFTE) process is a conventional counterpart of the HRFTE process without hydrostatic pressure which was shown schematically in Fig. 1e. As shown in Fig. 4b, the required load of the radial forward tube extrusion (RFTE) process is increased to about 1180 kN (for 350 mm billet length) from 89.9 kN (for 35 mm billet length). In other words, when the billet length increases by a factor of 10, the load of the RFTE process increases by a factor of 13.1. However, it is seen that the required loads of the HRFTE process with hydrostatic pressure for both 35-mm- and 350-mm-long tubes are the same and equal to 71.1 kN. This means that the HRFTE process with hydrostatic pressure is independent of the billet length. While in the RFTE process (without hydrostatic pressure), by increasing the length of the tube, the required load is sharply increased. A similar trend may be found in large-diameter billets. According to the Pascal principle, the pressure is linearly proportional to the force and is inversely proportional to the effective area. The required pressure is inversely proportional to the square of the effective diameter. Thus, the rate of increase in the force required for deformation is not larger than the rate of the effective area increase. So, the required hydrostatic pressure reduces by increasing the billet diameter. This is also true for the hydrostatic pressure required for the processing of a tube of the same dimension as that of the experiment test and for the processing of large-scale size with

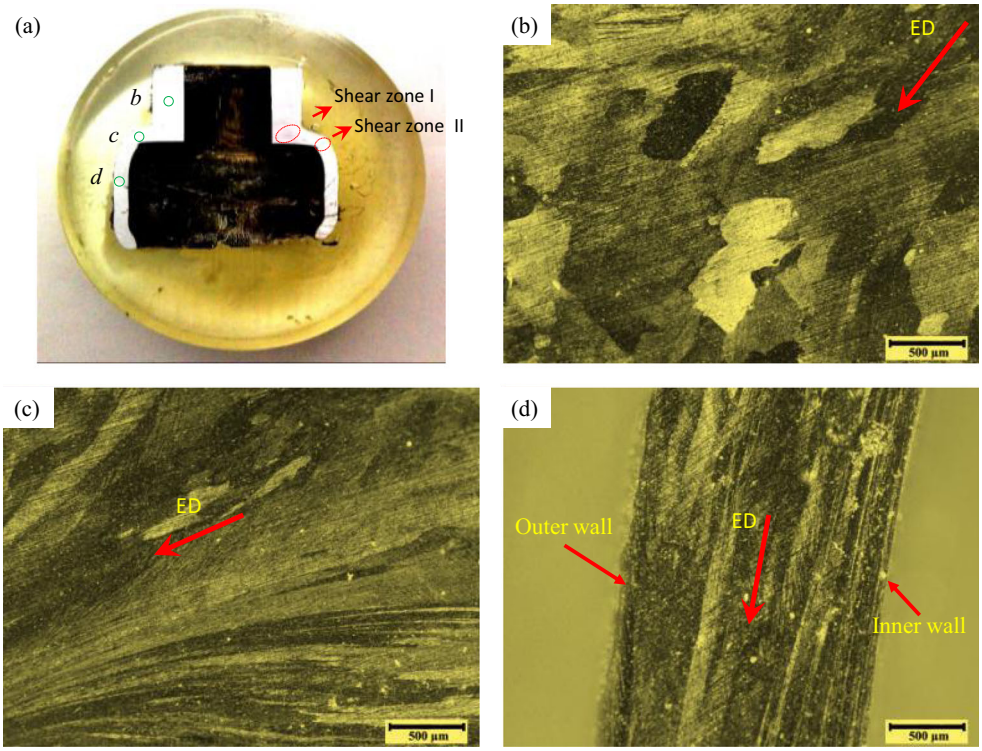

Fig. 6 **a** A cut section of the processed workpiece parallel to the longitudinal axis during the process. **b–d** Material flow microstructure of the HRFTE-processed sample (zones *b–d* as shown in **a**)

220 mm diameter of the initial billet and 320 mm diameter of the final tube (10 times larger). The maximum required force for the small size is 71.1 kN, and this hydrostatic pressure is equal to 1871 bar. However, the maximum required force for the large size is 6820 kN and leads to a hydrostatic pressure of 1795 bar. Therefore, the required hydrostatic pressure in the HRFTE process reduces by increasing the tube diameter. However, in other processes for producing a seamless tube, with an increase in the diameter, the force required increases and leads to the limitation of the production of seamless tubes with large diameters. However, the HRFTE process provides the conditions for reducing the hydrostatic pressure in the production of a seamless tube and also decreases the hydrostatic pressure with increasing size of the tube. So, the HRFTE process can be a suitable method with industrialization capabilities for producing large-diameter and long seamless tubes using a low capacity and small presses.

In the HRFTE process, unlike the conventional radial forward tube extrusion (RFTE), the initial billet is hollow. The required force reduces when using the hollow billet by eliminating the dead metal zone in the center of the billet and reducing the volume of material deformed. Figure 5 shows the FEM calculated force versus ram displacement for the HRFTE and conventional radial forward tube extrusion processes. As shown in Fig. 5, using the initial hollow billet instead of the solid one reduces the required load to about 45 %.

In the HRFTE process, a movable punch is put into the initial hollow billet. As mentioned earlier, when using the hydrostatic pressure and movable punch simultaneously, the effective area of hydrostatic pressure increases significantly in comparison with the case that a fixed punch is used inside the billet. So, considering the total force to be equal for two cases, the required hydrostatic pressure is reduced significantly (Pascal principle). As shown in Fig. 3, the maximum required force and corresponding hydrostatic pressure are, respectively, about 67.9 kN and 1787 bar. However, when instead of the movable punch, the fixed punch is used inside the initial billet, the hydrostatic pressure will increase to about 3003 bar as a result of effective area reduction. In other words, the required hydrostatic pressure for the same tube production increases about 170 %. In fact, the movable punch plays the main role and provides the possibility to produce seamless tubes under low hydrostatic pressure. This may be considered as an important advantage of HRFTE.

Figure 6a shows a cut section of the workpiece parallel to the longitudinal axis during the process. As shown, a hollow thick-walled tube is deformed to a thinner tube after extruding from two angular channels experiencing high shear deformation in zones I and II. The microstructures of the regions of "b," "c," and "d" (Fig. 6a) are shown, respectively, in panels b, c, and d of Fig. 6. The microstructure of region b that experiences no shear deformation with only constrained compression [27] is almost identical to the unprocessed recrystallized equiaxed microstructure with a grain size of about 350 μm. Material flow microstructure during the HRFTE process in the primary channel where the entrance of the radial channel (region c) is shown in Fig. 6c that shows stretching of the material structure with elongated grains along the almost extrusion direction. High compressive and shear strains that resulted from shear zone "I" is applied to the material in this zone. As shown, due to high compressive stress, the stretching rate near the mandrel is more than that of other regions [28]. The large effective strain is applied to the flow material at the entrance of the radial and forward channels in which the majority of this effective strain is in shear mode. The equivalent effective strain is increased with entrance of the flow material into the forward channel as a result of experiencing shear zone "II." The total accumulated equivalent plastic strain in zone d is about 2.56 (FEM). This causes more grain refinement and

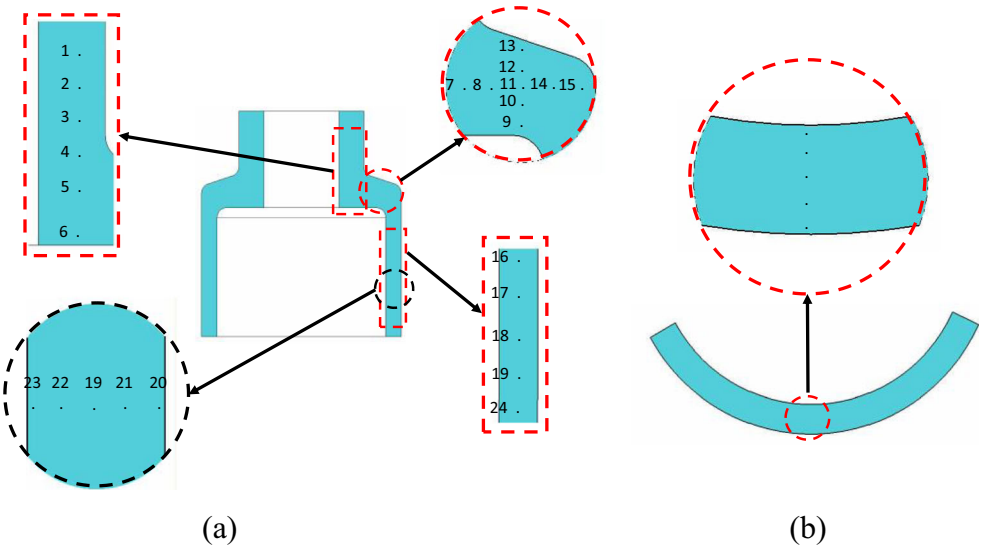

Fig. 7 Positions where the microhardness was measured in the cross section parallel to the axis (**a**) and perpendicular to the axis (**b**)

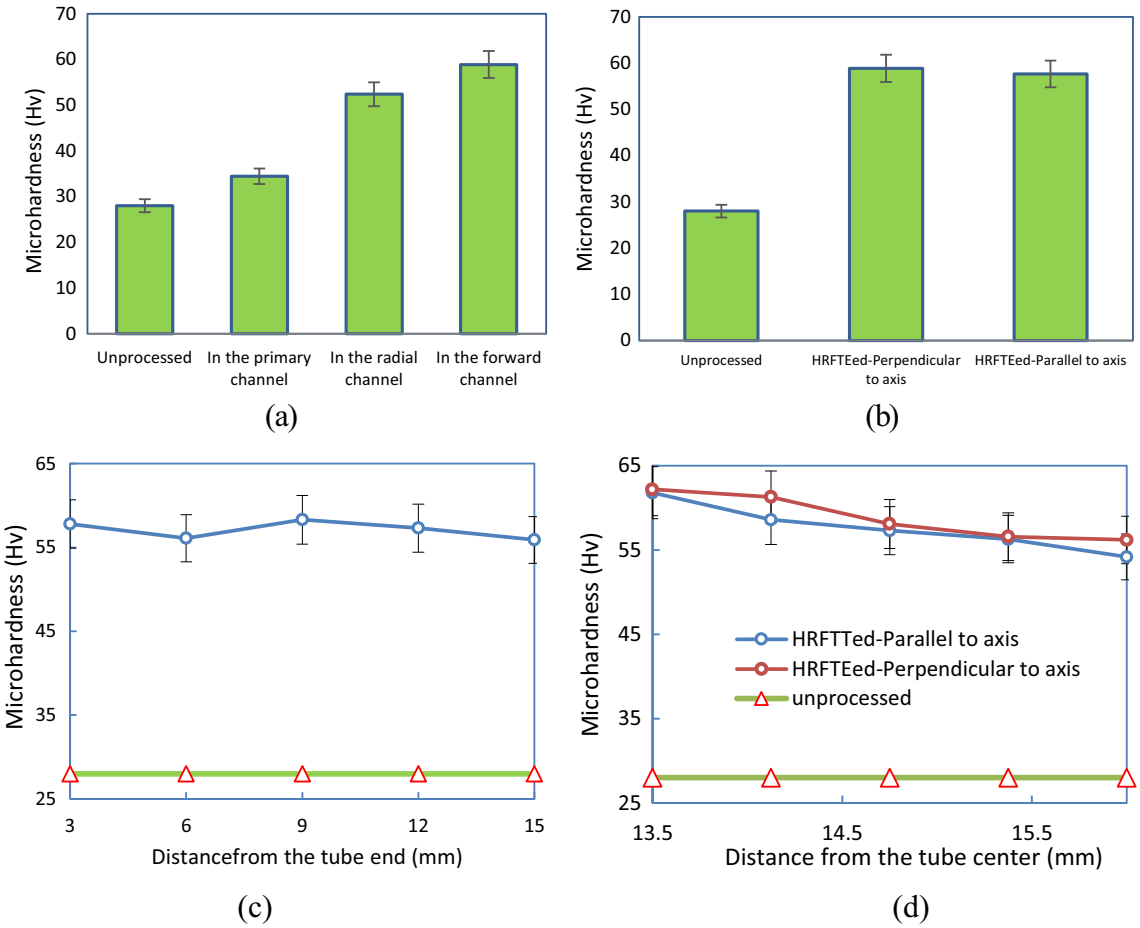

Fig. 8 **a** Microhardness changes at the different stage of the HRFTE process, **b** microhardness changes before and after the HRFTE process, **c** microhardness versus distance from HRFTE-processed tube end (along the points *16–19* in Fig. 7a), and **d** changes in microhardness along the tube thickness

microstructure stretching as shown in Fig. 6d. Then, the material is extruded in the 90° annular channel and the tube forms around the mandrel. Shear strain caused refinement of the grains and increased dislocations in the microstructure [29–32]. According to the figures, the HRFTE process caused significant grain refinement and grain elongation. The HRFTE process is a combined extrusion in which sequential radial extrusion and forward extrusion were performed. Also, producing a large seamless tube from a small initial hollow billet causes implementation of a large effective strain to the processed tube that leads to a significant grain refinement and improvement of the strength of the product.

Microhardness changes were studied at different sites of the aluminum workpiece during the HRFTE process as shown in Fig. 7a, b. Microhardness of the unprocessed aluminum was about 28 Hv. Figure 7a displays the points of the sample cross section parallel to axis direction where the microhardness was measured.

Microhardness change of material in the primary channel, before it enters the radial channels, is negligible because almost no microstructural changes occurred. Only in the primary channel and near the mandrel (point "6" in Fig. 7a), due to very high compressive and contact strains where the material starts to flow into the radial channel, was the

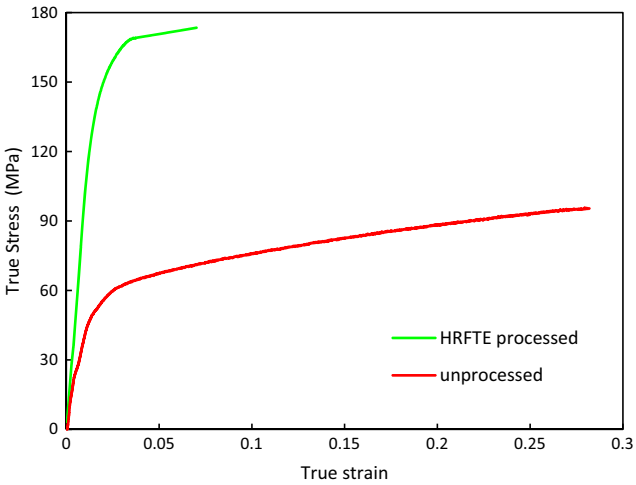

Fig. 9 True stress versus true strain of the unprocessed and final tube after the HRFTE process

Table 1 YS, UTS, and ductility of HRFTE-processed tube in comparison with those from SPD methods

Processing method	Effective strain	Strain rate (S^{-1})	YS (MPa)	UTS (MPa)	Ductility (%)	Reference
HRFTE	2.56	10^{-4}	154	176	7 %	This study
ECAP	~3	–	~130	~160	–	[43]
TCP	~2.5	–	85	160	6 %	[38]
CFS	2.25	10^{-5}	135	144	5 %	[37]
ASB	~2	–	~148	~190	8 %	[12]
CGP	~2.4	1.67×10^{-2}	~98	~108	–	[39]

microhardness slightly increased. The microhardness in the radial channel compared to that in the primary channel (in the 7–14 points in Fig. 7a) increases because the plastic strain was applied to the material and grain refinement, and work hardening occurs [32]. Microhardness was ~52.4 Hv, which is an average of the hardness values of points "9–13" in Fig. 7a.

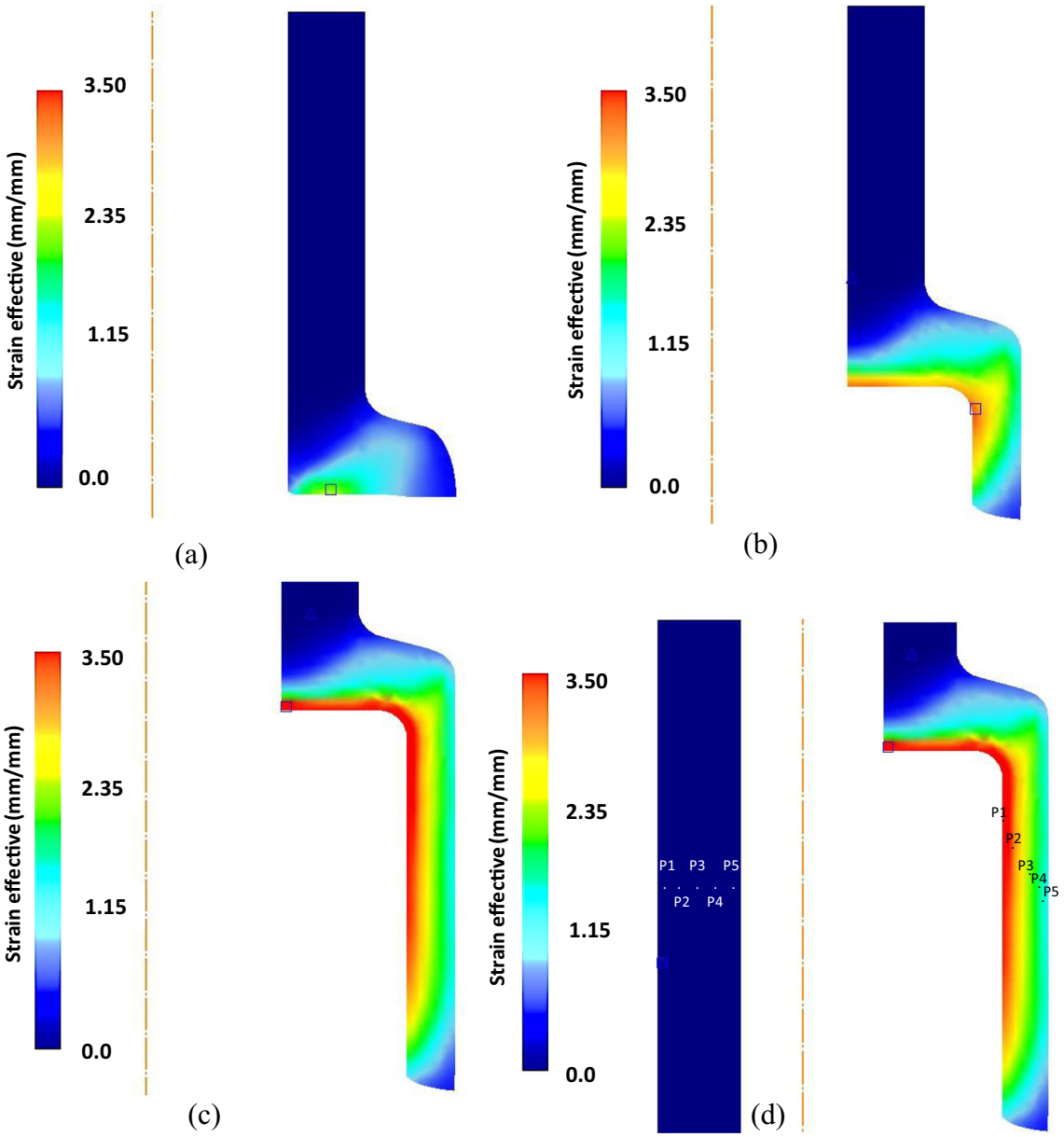

Fig. 10 **a**–**c** Effective plastic strain contours at different stages of HRFTE and **d** the selected nodes in the specimen, before and after the HRFTE process

Figure 8a shows the microhardness of the material at the different stage of the HRFTE process. Also, the hardness in the cross sections parallel and perpendicular to the axis are shown in Fig. 8b. Microhardness in the final tube was greater than that in other regions because this area experiences maximum effective strain.

The final tube microhardness (the hardness values of points 19–23 in Fig. 7a) was ~57.64 Hv that shows an enhancement factor of ~2.06 compared to that of unprocessed billet. The value of 2.06 is higher than that obtained in other tube SPD processes like TCAP and TCP processes. The values of about 1.53 after three passes of TCAP and about 1.7 after five passes of TCP [32, 33] were reported. Figure 8c shows microhardness variation across the length of the tube (points 16–19 and 24 in Fig. 7a). Microhardness along the length of the tube has good homogeneity and represents homogeneous properties along the tube. Microhardness changes across the thickness of the tube parallel (points 19–23 in Fig. 7a) and perpendicular (Fig. 7b) to axis directions are shown in Fig. 8d. The microhardness from the inner to the outer wall was slightly decreased because of the microstructural variations. In fact, there is an inhomogeneity in the properties of the tube along the thickness.

Figure 9 shows the true stress-strain curves of unprocessed and processed tubes. The HRFTE process increases the yield strength (YS) and ultimate strength (US) to 154 and 176 MPa, respectively, from 62 and 96 MPa. Rising in the yield strength and ultimate strength was due to grain refinement as a result of severe deformation applied in shear zones I and II in the entrance of the radial and forward channels together with high hydrostatic compressive stresses. Table 1 shows YS, UTS, and ductility of the HRFTE-processed tube in comparison with those from SPD methods. It is seen that relatively higher strength and ductility may be obtained in the HRFTE process in comparison with SPD methods. This may be achieved because of implementation of a high hydrostatic compressive stress when shear straining. Higher hydrostatic compressive stress is a vital factor for severe straining processes eliminating crack initiation and propagation [34, 35]. Also, it causes the formation of UFG and NG structures with high-angle grain boundaries which is an important characteristic of effective SPD methods [36]. As shown in Table 1, the methods with low hydrostatic pressures like cyclic flaring and sinking (CFS) [37], tube channel pressing (TCP) [38], and constrained groove pressing (CGP) [39] resulted in relatively low-strength materials. However, the processes with high hydrostatic compressive stress like HRFTE, HE [40], HPT [41], and ECAP with back pressure [42] and ASB [12] may produce high-strength ductile metals.

The effective strain contours at different stages of the HRFTE process are shown in Fig. 10a–c. In the HRFTE process, the material experiences compressive normal strains (resulting from the channel thickness reduction), tensile normal strains (resulting from an increase in the tube diameter), and shear strains (resulting from shear zones I and II). All these strains accumulated to the final tube material. As is seen in Fig. 10a, severe deformation occurs when the material starts to flow into the entrance of the radial channel. According to Fig. 10b, c, when the material flows into the forward channel, intense plastic deformation is applied as a result of the accumulated shear strains implemented in shear zones I and II. Because of high compressive stress on the inner wall of the tube, effective strain applied in these regions is greater than that in other regions. Figure 11a, b shows the change of effective strain at the selected nodes of p1–p5. As is seen, the effective strain in the inner wall of the tube is more than that in other regions. When moving to the outer wall, the effective strain is reducing so there would be some inhomogeneity through the cross section of the tube. This issue appeared in the material flow that was seen in Fig. 6b–d. This issue is also validated by changes of microhardness in Fig. 8d. From Fig. 10a, the average of the effective strain in the HRFTE process is about 2.56. That amount is comparable with most of the SPD methods at the end of the first pass. For TCAP [13] and TCEE [16] which are suitable SPD processes for the tubes, the values of average effective strain are, respectively, 2.67 and 1.92. As is realized, the HRFTE process

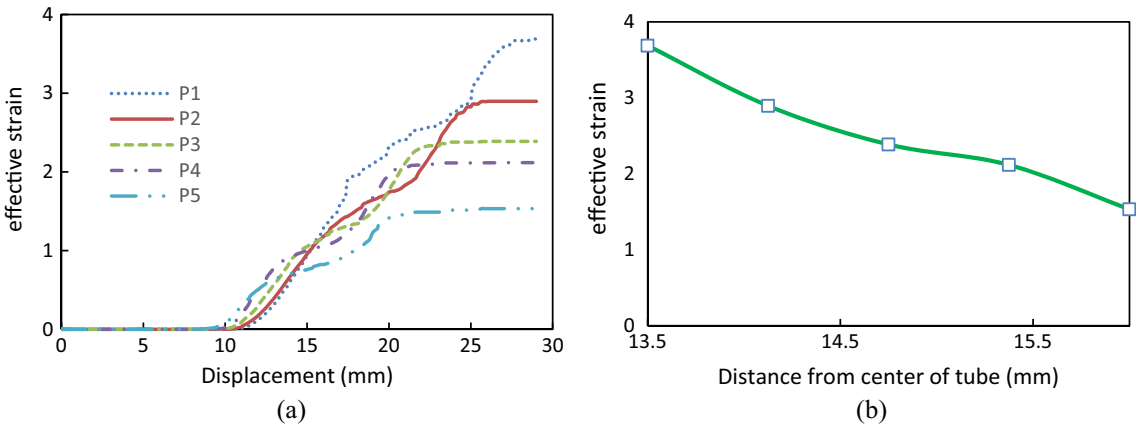

Fig. 11 **a** Effective plastic strain curves correspond to selected nodes in Fig. 10d, **b** path plot of the effective plastic strain from inside to the outside wall of the processed tube

significantly improves the strength of the tube by applying high plastic strains while applying higher hydrostatic stresses. Both of them are necessary for producing UFG and nanograined materials with high-angle grain boundaries [44, 45]. So, the strength improvement of the HRFTE process is comparable with that achieved by other SPD methods. Besides, the power required to carry out this process is low and, also, industrial capabilities for the production of large-diameter seamless tubes with superior mechanical properties using low hydrostatic pressure exist.

5 Conclusions

HRFTE was developed for processing seamless tubes with larger diameter from small initial hollow billets. Seamless aluminum tubes were successfully produced, and the mechanical properties and microstructure were investigated. The FEM was employed to show the advantages and study the deformation behavior. The following results could be concluded:

- HRFTE is a suitable process for producing larger seamless tubes from small hollow billets while using low pressures.
- Using hydrostatic pressure, the total force reduces about 20.9 %. When the billet length increases, the reduction factor sharply increases.
- When the billet length increases by a factor of 10, the load of the RFTE process (without hydrostatic pressure) increases by a factor of 13.1. However, it is seen that the required loads of the HRFTE process with hydrostatic pressure for both 35-mm- and 350-mm-long tubes are the same and are equal to the load of 35 mm.
- The movable punch plays the main role and provides the possibility to produce seamless tubes under low hydrostatic pressure.
- Using an initial hollow billet in this method reduced the force required about 43 %.
- With the enlargement of the billet diameter, the required hydrostatic pressure reduces.
- The average effective strain of 2.56 was achieved.
- Yield strength, ultimate strength, and microhardness were increased about 2.48, 1.92, and 2.1 times compared to the initial value, respectively.

References

1. Buschhausen A, Weinmann K, Lee JY, Altan T (1992) Evaluation of lubrication and friction in cold forging using a double backward-extrusion process. J Mater Process Technol 33:95–108. doi:10.1016/0924-0136(92)90313-H
2. Cho HY, Min GS, Jo CY, Kim MH (2003) Process design of the cold forging of a billet by forward and backward extrusion. J Mater Process Technol 135:375–381. doi:10.1016/S0924-0136(02)00870-1
3. Shatermashhadi V, Manafi B, Abrinia K, Faraji G, Sanei M (2014) Development of a novel method for the backward extrusion. Mater Des 62:361–366. doi:10.1016/j.matdes.2014.05.022
4. Lee Y, Hwang S, Chang Y, Hwang B (2001) The forming characteristics of radial–forward extrusion. J Mater Process Technol 113:136–140. doi:10.1016/S0924-0136(01)00705-1
5. Robertson J (1894) Method of and apparatus for forming metal articles, British Patent No. 19 356 (October 14, 1893). US Patent (524):504
6. Skiba J, Pachla W, Mazur A, Przybysz S, Kulczyk M, Przybysz M, Wróblewska M (2014) Press for hydrostatic extrusion with back-pressure and the properties of thus extruded materials. J Mater Process Technol 214:67–74. doi:10.1016/j.jmatprotec.2013.07.014
7. Bridgman PW (1952) Studies in large plastic flow and fracture, vol 177. McGraw-Hill New York
8. Faraji G, Jafarzadeh H, Jeong H, Mashhadi M, Kim H (2012) Numerical and experimental investigation of the deformation behavior during the accumulative back extrusion of an AZ91 magnesium alloy. Mater Des 35:251–258. doi:10.1016/j.matdes.2011.09.057
9. Xie JX, Ikeda K, Murakami T (1995) UBA analysis of the process of pipe extrusion through a porthole die. J Mater Process Technol 49(3–4):371–385. doi:10.1016/0924-0136(94)01582-L
10. Wang JT, Li Z, Wang J, Langdon TG (2012) Principles of severe plastic deformation using tube high-pressure shearing. Scr Mater 67(10):810–813. doi:10.1016/j.scriptamat.2012.07.028
11. Arzaghi M, Fundenberger J, Toth L, Arruffat R, Faure L, Beausir B, Sauvage X (2012) Microstructure, texture and mechanical properties of aluminum processed by high-pressure tube twisting. Acta Mater 60(11):4393–4408. doi:10.1016/j.actamat.2012.04.035
12. Mohebbi MS, Akbarzadeh A (2010) Accumulative spin-bonding (ASB) as a novel SPD process for fabrication of nanostructured tubes. Mater Sci Eng A 528(1):180–188. doi:10.1016/j.msea.2010.08.081
13. Faraji G, Mashhadi MM, Kim HS (2011) Tubular channel angular pressing (TCAP) as a novel severe plastic deformation method for cylindrical tubes. Mater Lett 65(19):3009–3012. doi:10.1016/j.matlet.2011.06.039
14. Faraji G, Babaei A, Mashhadi MM, Abrinia K (2012) Parallel tubular channel angular pressing (PTCAP) as a new severe plastic deformation method for cylindrical tubes. Mater Lett 77:82–85. doi:10.1016/j.matlet.2012.03.007
15. Faraji G, Mashhadi M, Bushroa A, Babaei A (2013) TEM analysis and determination of dislocation densities in nanostructured copper tube produced via parallel tubular channel angular pressing process. Mater Sci Eng A 563:193–198. doi:10.1016/j.msea.2012.11.065
16. Babaei A, Mashhadi MM, Jafarzadeh H (2014) Tube cyclic expansion-extrusion (TCEE) as a novel severe plastic deformation method for cylindrical tubes. J Mater Sci 49:3158–3165. doi:10.1007/s10853-014-8017-6
17. Chan WL, Fu MW, Yang B (2011) Study of size effect in micro-extrusion process of pure copper. Mater Des 32(7):3772–3782. doi:10.1016/j.matdes.2011.03.045
18. Faraji G, Mashhadi MM, Joo S-H, Kim HS (2012) The role of friction in tubular channel angular pressing. Rev Adv Mater Sci 31:12–18
19. Taylan Altan ERCNSMOSU, Gracious Ngaile NCSU, Gangshu Shen LCI (2004) Cold and hot forging: fundamentals and applications. Materials Park, Ohio
20. Hung J-c, Hung C (2000) The design and development of a hydrostatic extrusion apparatus. 104:226–235. doi:10.1016/S0924-0136(00)00593-8

21. Skiba J, Pachla W, Mazur A, Przybysz S, Kulczyk M, Przybysz M, Wróblewska M (2014) Press for hydrostatic extrusion with back-pressure and the properties of thus extruded materials. J Mater Proc Technol 214(1):67–74. doi:10.1016/j.jmatprotec.2013.07.014
22. Faraji G, Mashhadi MM, Kim HS (2011) Microstructure inhomogeneity in ultra-fine grained bulk AZ91 produced by accumulative back extrusion (ABE). Mater Sci Eng A 528(13–14):4312–4317. doi:10.1016/j.msea.2011.02.075
23. Tobias SA (1968) The design and development of a hydrostatic extrusion machine. 8:125–140
24. Hosseini SH, Abrinia K, Faraji G (2014) Applicability of a modified backward extrusion process on commercially pure aluminium. Mater Des. doi:10.1016/j.matdes.2014.09.043
25. Faraji G, Mashhadi MM, Kim HS (2012) Deformation behavior in tubular channel angular pressing (TCAP) using triangular and semi-circular channels. Mater Trans 53(1):8–12. doi:10.2320/matertrans.MD201107
26. Hung J-C, Hung C (2000) The design and development of a hydrostatic extrusion apparatus. J Mater Process Technol 104(3):226–235. doi:10.1016/S0924-0136(00)00593-8
27. Faraji G, Mashhadi M, Kim H (2011) Microstructure inhomogeneity in ultra-fine grained bulk AZ91 produced by accumulative back extrusion (ABE). Mater Sci Eng A 528(13):4312–4317. doi:10.1016/j.msea.2011.02.075
28. Thirumurugan M, Kumaran S (2013) Extrusion and precipitation hardening behavior of AZ91 magnesium alloy. Trans Nonferrous Metals Soc China (English Edition) 23 (6):1595–1601. doi:10.1016/S1003-6326(13)62636-9
29. Alihosseini H, Zaeem MA, Dehghani K, Shivaee HA (2012) Producing ultra fine-grained aluminum rods by cyclic forward-backward extrusion: study the microstructures and mechanical properties. doi:10.1016/j.matlet.2012.01.102
30. Haghdadi N, Zarei-Hanzaki A, Abou-Ras D (2013) Microstructure and mechanical properties of commercially pure aluminum processed by accumulative back extrusion. Mater Sci Eng A 584:73–81. doi:10.1016/j.msea.2013.06.060
31. Haghdadi N, Zarei-Hanzaki A, Abou-Ras D, Maghsoudi MH, Ghorbani A, Kawasaki M (2014) An investigation into the homogeneity of microstructure, strain pattern and hardness of pure aluminum processed by accumulative back extrusion. Mater Sci Eng A 595:179–187. doi:10.1016/j.msea.2013.11.077
32. Mesbah M, Faraji G, Bushroa AR (2014) Characterization of nanostructured pure aluminum tubes produced by tubular channel angular pressing (TCAP). Mater Sci Eng A 590:289–294. doi:10.1016/j.msea.2013.10.036
33. Alihosseini H, Faraji G, Dizaji AF, Dehghani K (2012) Characterization of ultra-fine grained aluminum produced by accumulative back extrusion (ABE). Mater Charact 68:14–21. doi:10.1016/j.matchar.2012.03.004
34. Dieter GE, Kuhn HA, Semiatin SL (2003) Handbook of workability and process design. ASM international
35. Estrin Y, Vinogradov A (2013) Extreme grain refinement by severe plastic deformation: a wealth of challenging science. Acta Mater 61(3):782–817. doi:10.1016/j.actamat.2012.10.038
36. Xu C, Horita Z, Langdon TG (2007) The evolution of homogeneity in processing by high-pressure torsion. Acta Mater 55(1):203–212. doi:10.1016/j.actamat.2006.07.029
37. Torabzadeh H, Faraji G, Zalnezhad E (2016) Cyclic flaring and sinking (CFS) as a new severe plastic deformation method for thin-walled cylindrical tubes. Trans Indian Inst Metals. doi:10.1007/s12666-015-0685-7
38. Zangiabadi A, Kazeminezhad M (2011) Development of a novel severe plastic deformation method for tubular materials: tube channel pressing (TCP). Mater Sci Eng A 528(15):5066–5072. doi:10.1016/j.msea.2011.03.012
39. Satheesh Kumar SS, Raghu T (2015) Strain path effects on microstructural evolution and mechanical behaviour of constrained groove pressed aluminium sheets. Mater Des 88:799–809. doi:10.1016/j.matdes.2015.09.057
40. Lewandowska M, Kurzydlowski KJ (2008) Recent development in grain refinement by hydrostatic extrusion. J Mater Sci 43:7299–7306. doi:10.1007/s10853-008-2810-z
41. Zhilyaev AP, Langdon TG (2008) Using high-pressure torsion for metal processing: fundamentals and applications. Prog Mater Sci 53(6):893–979. doi:10.1016/j.pmatsci.2008.03.002
42. Xu C, Xia K, Langdon TG (2007) The role of back pressure in the processing of pure aluminum by equal-channel angular pressing. Acta Mater 55(7):2351–2360. doi:10.1016/j.actamat.2006.11.036
43. Raab GJ, Valiev RZ, Lowe TC, Zhu YT (2004) Continuous processing of ultrafine grained Al by ECAP–conform. Mater Sci Eng A 382(1–2):30–34. doi:10.1016/j.msea.2004.04.021
44. Zehetbauer MJ, Stüwe HP, Vorhauer A, Schafler E, Kohout J (2003) The role of hydrostatic pressure in severe plastic deformation. Adv Eng Mater 5:330–337. doi:10.1002/adem.200310090
45. Pachla W, Kulczyk M, Sus-Ryszkowska M, Mazur A, Kurzydlowski KJ (2008) Nanocrystalline titanium produced by hydrostatic extrusion. J Mater Process Technol 205:173–182. doi:10.1016/j.jmatprotec.2007.11.103